

Deformation behaviour in α/β two-phase superplastic brass

DING HUA, WU QINGLING, MA LONGXIANG

Box 317, Northeast University of Technology, Shenyang, Liaoning, People's Republic of China

α/β brass consists of hard α and soft β phase in its superplastic temperature range. Because of the difference between their mechanical properties, the superplastic behaviour of the alloy differs from that of other single-phase and quasi-single-phase alloys. The mechanical properties and microstructure of leaded α/β brass during superplastic deformation were studied and the mechanism is discussed. It is shown that the boundary diffusion controls the superplastic deformation process and boundary sliding is the main deformation mechanism; there is little deformation in the α -phase, and intragranular slip as the accommodating mechanism mainly occurs in β -phase in the superplastic range. It is also shown that the bulk diffusion dominates the deformation process, and intragranular slip is the main mechanism in the non-superplastic range.

1. Introduction

In recent years, the superplasticity of α/β brass has been widely studied. Many works have been performed on the superplastic pre-treatment and deformation conditions, superplastic deformation mechanism and cavitation during superplastic deformation in the alloys [1-8].

Because the mechanical properties of α and β phases of brass are quite different in superplastic deformation, the superplastic behaviour of α/β brass is different from that of other single-phase or quasi-single-phase alloys. There are two view-points in the deformation mechanism of α/β brass. One is that the slip in the β -phase dominates the superplastic deformation [9], and the other is that the boundary sliding accommodated by the slip is the main deformation mechanism [10]. Up to now, however, there has been no sufficient evidence for either viewpoint. The aim of this work was to study the deformation behaviour of α/β brass in the superplastic and non-superplastic ranges, and by measuring the strains in α - and β -phases to determine the deformation mechanisms.

2. Experimental procedure

2.1. Superplastic pre-treatment and tensile tests

The alloy chosen was 59-1 leaded brass with 59% Cu, 1% Pb and zinc the balance. The superplastic pre-treatment process was as follows. Hot-rolled plates (6 mm thick) were solution-treated (800 °C/40-60 min), rolled to 3 mm and annealed (600 °C/30-50 min), then rolled to 1.5 mm and annealed (500 °C/30-50 min) and finally rolled to 1 mm thick.

The tensile specimens were cut directly from the cold-rolled sheets with a gauge length of 10 mm, the direction of which is parallel to the rolling direction.

2.2. Surface observation

Scratches perpendicular to the gauge length were made on the polished surface by a grating scratch machine. The specimens were elongated by 30% at 525 °C and the strain rates $8.33 \times 10^{-4} \text{ s}^{-1}$ and $8.33 \times 10^{-2} \text{ s}^{-1}$, respectively, in high pass-by argon atmosphere.

The spacings between marker lines in α and β grains before and after the deformation were measured under an optical microscope. A total of 75 measurements were made.

3. Results

3.1. Mechanical properties

The material treated by the process mentioned in Section 2.1 exhibits 550% maximum elongation at 600 °C and a strain rate of $8.33 \times 10^{-4} \text{ s}^{-1}$.

Fig. 1 shows the $\log \sigma$ - $\log \dot{\epsilon}$ relationships at 500 and 600 °C. The strain-rate sensitivity coefficient, m , is determined as a function of strain rate at 600 °C (Fig. 2), using the method proposed by Backofen *et al.* [11]. Taking m as greater than 0.3 as the superplastic region, the superplastic strain-rate range is from 1.67×10^{-4} - $8.33 \times 10^{-2} \text{ s}^{-1}$ at 600 °C. Being calculated from the $m^{-1} \log \sigma - 1/T$ relationship (Fig. 3), the activation energies at optimum superplastic strain rate and non-superplastic strain rate, are 62 and $120 \text{ kJ mol}^{-1} \text{ K}^{-1}$, respectively.

3.2. Microstructure

Fig. 4 shows the microstructures of specimens investigated (white is α -phase). Because the specimens were as-rolled in the beginning, the grains were of an elongated shape (Fig. 4a). After holding for 10 min at 600 °C, most of them changed to equiaxed structure (Fig. 4b). When the specimens were deformed at strain

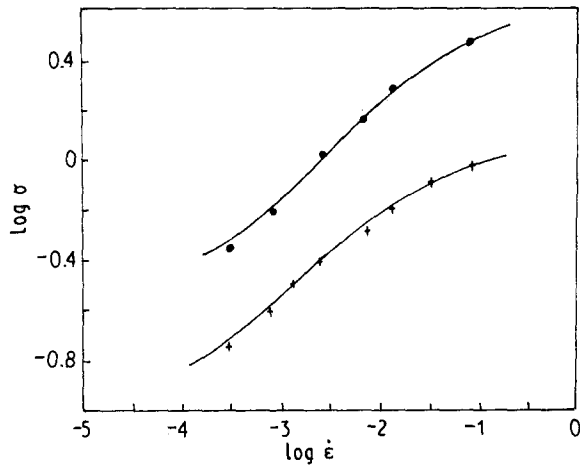


Figure 1 Logarithmic plot of flow stress against strain rate at (●) 500 and (+) 600 °C.

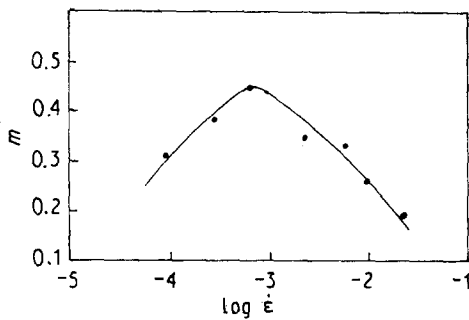


Figure 2 Dependence of m on strain rate at 600 °C.

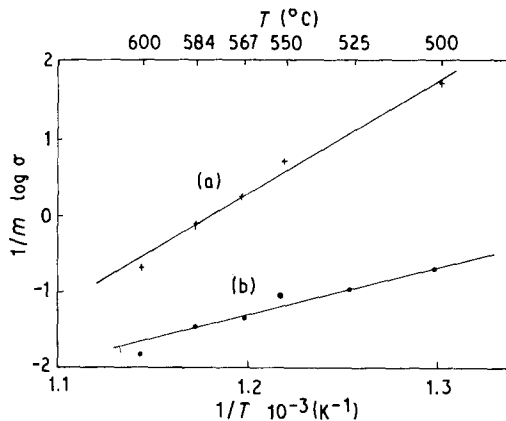


Figure 3 Dependence of $1/m \log \sigma$ on $1/T$, for $\dot{\epsilon}_0 = (+)$ $4.167 \times 10^{-2} \text{ s}^{-1}$, (●) $8.33 \times 10^{-4} \text{ s}^{-1}$. $Q = (a)$ $120 \text{ kJ mol}^{-1} \text{ K}^{-1}$, (b) $62 \text{ kJ mol}^{-1} \text{ K}^{-1}$.

rates of 8.33×10^{-4} and $8.33 \times 10^{-2} \text{ s}^{-1}$ at 600 °C, and with 30% strain, no distinct grain growth was found (Fig. 4c and d). Finally, as the strain reached to 300%, grain coarsening occurred (Fig. 4e).

3.3. Intragranular slip

The strain due to the intragranular slip is estimated as

$$\epsilon_s = (d' - d)/d \quad (1)$$

where d and d' are spacings between marker lines in

the confines of one grain before and after deformation, respectively.

The results for $\epsilon_{s\alpha}$ and $\epsilon_{s\beta}$ are shown in Table I.

Suppose that the stresses in the two phases are the same, the average strain of the alloy due to the intragranular slip is given by

$$\bar{\epsilon}_s = f_\alpha \epsilon_{s\alpha} + f_\beta \epsilon_{s\beta} \quad (2)$$

where f_α and f_β are the volume fractions of the α - and β -phases, respectively. The slip contribution to the total strain, ζ_s , is estimated from the expression

$$\zeta_s = \bar{\epsilon}_s / \epsilon_{\text{tot}} \quad (3)$$

ζ_s was then 26.9% and 66.9% at 8.33×10^{-4} and $8.33 \times 10^{-2} \text{ s}^{-1}$, respectively.

Fig. 5a shows the microstructure of the specimen before deformation. Fig. 5b and c show those after deformation in the grip region and in the gauge length, respectively ($T = 525 \text{ °C}$, $\epsilon = 30\%$, $\dot{\epsilon} = 8.33 \times 10^{-2} \text{ s}^{-1}$). It can be seen that the spacing between the marker lines in the grip region remains the same after deformation (Fig. 5a and b). In the gauge length, the spacing between the marker lines does not change much in the α -phase, but it does show an obvious change in the β -phase (Fig. 5c).

4. Discussion

4.1. The rate-controlling process of superplastic deformation

It is difficult to measure the activation energy in the superplastic deformation of α/β brass accurately. In general, it can be supposed that the superplastic deformation is a thermal activation process. The strain rate is given by

$$\dot{\epsilon} = K' \sigma^{1/m} \exp(-Q/RT) \quad (4)$$

where K' is taken as a constant, which is determined by the structure and defect condition of the material. For brass, the α/β ratio varies as the temperature changes, so that K' is no longer a constant. This problem could be solved by comparing the activation energy in superplastic and non-superplastic conditions. In our experiment, the activation energy of superplastic deformation was just half of that of the non-superplastic deformation. It is well-known that the non-superplastic deformation process is controlled by bulk diffusion and that the activation energy of boundary diffusion is half of that of bulk diffusion. Therefore, it could be concluded that the boundary diffusion controls the superplastic deformation process in α/β brass.

4.2. The main deformation mechanism in superplastic range II

There are two interpretations of the superplastic deformation mechanism of α/β brass. One is that the slip in the β -phase dominates the superplastic deformation [9], and the other is that the boundary sliding accommodated by the slip is the main superplastic deformation mechanism [10]. Up to now, however, insufficient evidence has been provided for both viewpoints.

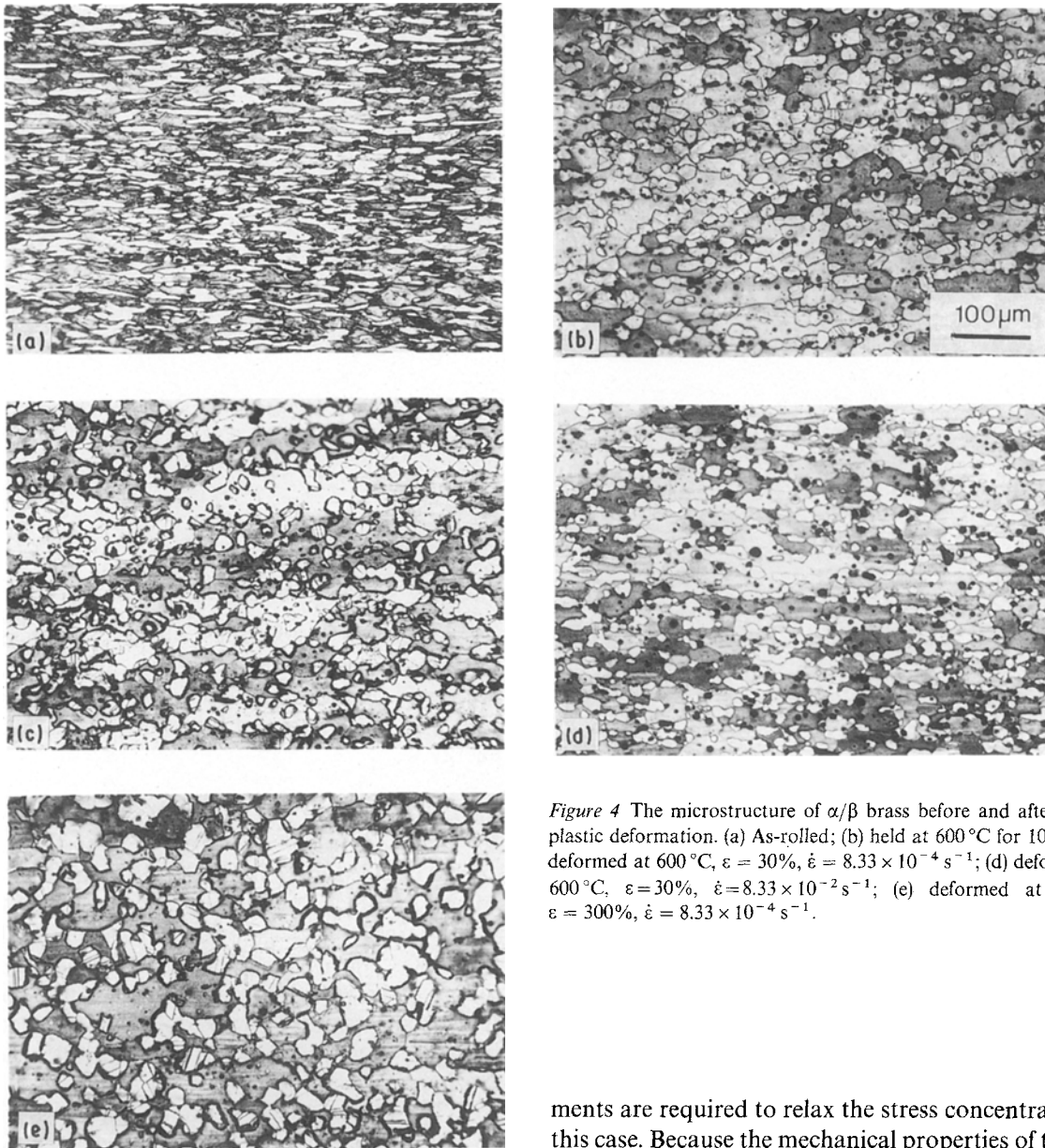


Figure 4 The microstructure of α/β brass before and after superplastic deformation. (a) As-rolled; (b) held at 600 °C for 10 min; (c) deformed at 600 °C, $\epsilon = 30\%$, $\dot{\epsilon} = 8.33 \times 10^{-4} \text{ s}^{-1}$; (d) deformed at 600 °C, $\epsilon = 30\%$, $\dot{\epsilon} = 8.33 \times 10^{-2} \text{ s}^{-1}$; (e) deformed at 600 °C, $\epsilon = 300\%$, $\dot{\epsilon} = 8.33 \times 10^{-4} \text{ s}^{-1}$.

TABLE I Strains due to slip

$\dot{\epsilon}_0(\text{s}^{-1})$	$\epsilon_{s\alpha}(\%)$	$\epsilon_{s\beta}(\%)$
8.33×10^{-4}	2.13	15.10
8.33×10^{-2}	7.60	30.80

Our experiment shows that there is little deformation in the α -phase and that the strain of the β -phase due to slip is 26.9%. These results indicated that intragranular slip is not the main mechanism in the superplastic range II. Boundary sliding in superplastic deformation of α/β brass was observed [6]. It was found that much boundary sliding occurred and the boundary sliding rate is the highest on the α/β boundaries. Therefore, it could be concluded that boundary sliding is the main deformation mechanism in the superplastic range II.

When boundary sliding meets obstacles, stress concentration would occur, so that dislocation move-

ments are required to relax the stress concentration in this case. Because the mechanical properties of the two phases are very different in the superplastic deformation range, the accommodation process is also different from single phase and quasi-single-phase alloys. Thus the superplastic deformation model suggested by Mukherjee [12] should be modified.

In the temperature range 500–600 °C, the critical resolved shear stress of the β -phase is much lower than that of the α -phase so that the slip accommodation of the boundary sliding occurs first in the β -phase. Fig. 6 is a schematic illustration of the accommodation process modified from Mukherjee's model. In the superplastic deformation range the α/β ratio is approximately equal to one, and the boundary sliding mostly occurs on the α/β interphase, thus only interfacial sliding is considered.

The dislocations generated at the interphase boundary ledges slip and pile up along the slip plane at the opposite interphase boundary. The dislocations at the head of a pile-up can climb into and along the interphase boundary to the annihilation sites. The deformation rate is then controlled by the dislocation climbing rate. This is consistent with the activation energy measurement which indicates that the boundary diffusion controls the superplastic deformation process.

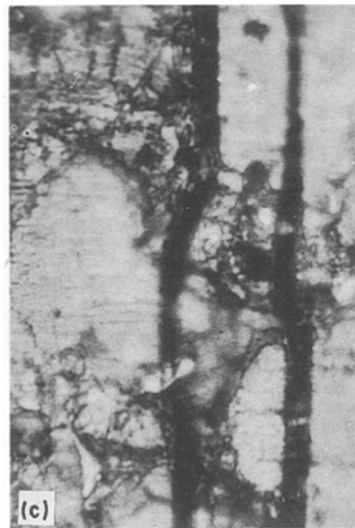
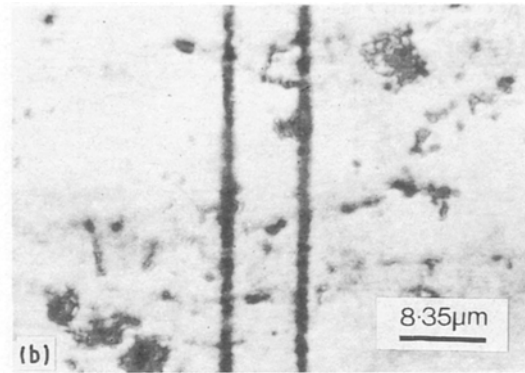
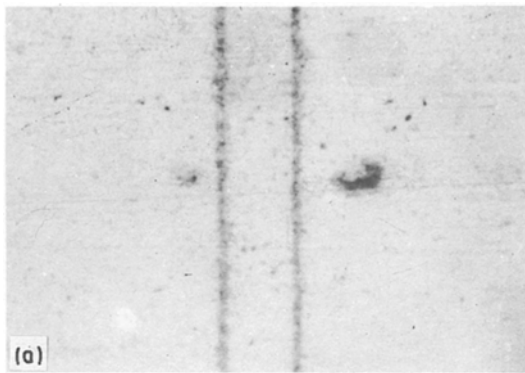


Figure 5 Surface observation of the marker lines (a) before deformation and (b) after deformation in the grip region and (c) in the gauge length. $T = 525^\circ\text{C}$, $\epsilon = 30\%$, $\dot{\epsilon} = 8.33 \times 10^{-2} \text{ s}^{-1}$.

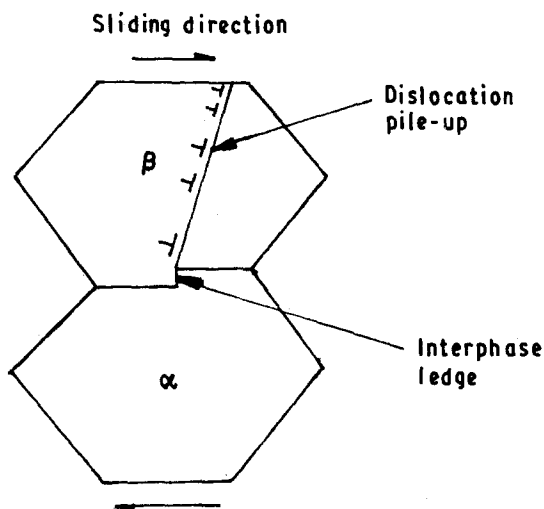


Figure 6 Schematic representation of boundary sliding accommodated by slip in the β -phase

4.3. The main deformation mechanism in non-superplastic range III

In range III, slip systems in the α -phase are also initiated and some extent of slip occurs in it. A great deal of slip occurs in the β -phase. The intragranular slip is the main deformation mechanism. Because much slip occurs in range III, dislocations in different slip systems would intersect and jog each other and Lomer-Cottrell dislocations would be formed.

The moving dislocations would pile up at these obstacles and stress concentration would occur; therefore, bulk diffusion dominates the deformation process. This is also verified by the measured activation energy.

5. Conclusions

1. 59-1 leaded brass has 550% elongation at 600°C and $8.33 \times 10^{-4} \text{ s}^{-1}$. The maximum of m is 0.43.

2. In superplastic range II, boundary diffusion dominates the deformation process and boundary sliding is the main deformation mechanism. In non-superplastic range III, bulk diffusion dominates the deformation process and intragranular slip is the main deformation mechanism.

3. The α - and β -phases show different behaviour because of the difference in their mechanical properties. In superplastic deformation there is little slip in the α -phase, and intragranular slip as the accommodating mechanism occurs mainly in the β -phase. At higher strain rate, there is some intragranular slip in the α -phase and there is a great deal of slip in the β -phase.

References

1. S. SAGAT, P. BLENKISOP and D. M. R. TAPLIN, *J. Inst. Metals* **100** (1972) 268.
2. M. SUERY and B. BAUDELET, *J. Mater. Sci.* **8** (1973) 363.
3. J. W. P. PATTERSON, *ibid.* **16** (1981) 457.
4. C. W. HAMPHRIES and N. RIDLEY, *ibid.* **13** (1978) 2477.
5. S. SAGAT and D. M. R. TAPLIN, *Acta Metall.* **24** (1976) 307.
6. T. CHANDRA, J. J. JONAS and D. M. R. TAPLIN, *J. Mater. Sci.* **13** (1978) 2380.
7. J. BELZUNCE and M. SUERY, *Scripta Metall.* **15** (1981) 895.
8. *Idem*, *Acta Metall.* **31** (1983) 1497.
9. M. SUERY and B. BAUDELET, *Res. Mech.* **2** (1981) 163.
10. V. G. BARO, *Z. Metallkde* **63** (1972) 384.
11. W. A. BACKOFEN *et al.*, *Trans. ASM* **57** (1964) 980.
12. AMIYA K. MUKHERJEE, *Mater. Sci. Engng* **8** (1981) 83.

Received 10 July 1990
and accepted 10 February 1991